Turkish Journal of Electrical Engineering & Computer Sciences

http://journals.tubitak.gov.tr/elektrik/

Research Article

Turk J Elec Eng & Comp Sci
(2017) 25: 3319 – 3333

doi:10.3906/elk-1604-410

High-voltage isolated multioutput power supply for multilevel converters

Amir SEPEHR[1], **Mehdi SARADARZADEH**[2,*], **Shahrokh FARHANGI**[1]
[1]School of Electrical and Computer Engineering, University of Tehran, Tehran, Iran
[2]Department of Electrical and Computer Engineering, Jundi Shapur University of Technology, Dezful, Iran

Received: 29.04.2016 • **Accepted/Published Online:** 02.01.2017 • **Final Version:** 30.07.2017

Abstract: Multilevel converters are one of the major choices for realizing high electric power conversion. The major feature of multilevel converter topologies is the need for a large number of switches, each of which requires a gate driver circuit and an isolated DC power supply. In this paper, a pragmatic concept of design and implementation of an isolated DC-to-DC converter for a high-voltage isolated application is introduced. More specifically, a multiple isolated output power supply based on the benefits of resonant converters is designed to prepare 36 double DC voltages for driving power semiconductor devices in a three-phase, seven-level cascaded H-bridge that acts as a static synchronous series compensator (SSSC). The power supply contains several high-frequency transformers in series, carrying a high-frequency single turn current as their primary winding excitations, and they are improved by a resonant tank circuit to reduce switching and core losses. The proposed design has a high voltage insulation level, low cost, small size, adequate hold-up time, and an easily upwards extending structure. The feasibility of the design is clarified by simulation results and implementation in a high-power D-SSSC converter.

Key words: Isolated DC power supply, multilevel converters, resonant converters, soft switching

1. Introduction

In many industrial applications, high-power semiconductor switches need a special power supply for their driver circuits that must be isolated from all other relevant potentials in the converter; this insulation requirement can generally be achieved by using expensive and bulky transformers. High-insulation transformers are used when high energy is necessary in the driver. These transformers provide energy to all types of applications [1]. Self-supplied drivers are also presented that use the switching periods of the semiconductors to obtain energy to supply the driver; however, they are only limited to specific applications [2,3]. Light-triggered devices require no external power supply to generate the gate pulse for the semiconductor, but these are only suitable for low-power applications [1,4]. Existing power supplies have major drawbacks that highlight the need for a new brand of isolated power supplies. The aim of this paper is to develop a general power supply for powering up all types of insulated gate bipolar transistor (IGBT) devices in medium-voltage applications such as inverters and rectifiers by considering the required insulation.

The resonant converter is a notable candidate for realizing small-size, high-efficiency isolated power supplies. Moreover, resonant converters have been successfully applied to various industrial, commercial, and domestic applications because of their interesting benefits such as zero-voltage switching (ZVS) and/or zero-current switching, high-frequency operation, high efficiency, small size, low electromagnetic interference, and

*Correspondence: saradar@jsu.ac.ir

low reverse-recovery losses in diodes [5–8]. In addition, different resonant converters demonstrate widely varying characteristics, indicating their suitability for special application. For instance, the output voltage of an LCL resonant converter is load-independent when it operates at resonant frequency, which makes it attractive as a constant-voltage power supply [5–9]. Similarly, in [10], and [11], a secondary-side phase-shift-controlled LLC resonant converter was introduced, which supports adequate hold-up time for applications such as distributed power systems and server power supplies. Another use of the resonant converter in such applications was proposed in [12], which presents the steady-state analysis of a fixed-frequency phase-shift LCLC resonant converter with a capacitive output filter for high-voltage applications. In [1] and [3], some other DC-to-DC converter topologies, which are used for designing power supplies with high-voltage insulations, were discussed.

In this paper, a high-frequency, soft-switched DC-to-DC converter is proposed that excels over the aforementioned power supplies and offers a higher voltage insulation level, lower cost, easier upward extension, more hold-up time, and simple implementation. Moreover, the high-frequency transformers in this converter do not need to be potted or put in an oil tank, and this greatly reduces cost and size. In order to show the feasibility of the proposed design, experimental implementation in an industrial three-phase, seven-level cascaded H-bridge converter, which acts as a distribution-level static synchronous series compensator (D-SSSC), is also presented. The paper is arranged as follows: in the next section, the application and the structure of the high-insulation power supply are introduced. Subsequently, circuit design principles are explained. The switching method and control strategy are then presented and, at the end, the simulation and experimental results of the proposed power supply are demonstrated.

2. Application and structure

Multilevel converters work well in high-power applications in comparison with conventional two-level inverters, and their use is rapidly spreading. Their many advantages, such as high power quality, lower harmonic components, better electromagnetic features, lower dv/dt, and lower switching losses, also make them popular in various industries. Furthermore, combining large numbers of semiconductor devices to achieve a high VA rating is well established in these converters [13,14]. The most applicable functionalities of multilevel converters are high-power rectifiers, DC-to-DC converters, large motor drives, and power system FACTS controllers [15,16].

The cascaded H-bridge, the neutral point clamped, and the flying capacitors are the most widely used topologies of multilevel inverters, all of which require $6 \times(m-1)$ switches to provide m-level output voltage [13,17]. To drive each switch, a pair of voltage supplies, positive and negative, are required. Due to the high voltage level and insulation requirements in medium-voltage inverters, providing a high number of isolated power supplies becomes more complex and costly. This paper proposes a practical converter scheme to provide isolated power supplies, which are low in cost and volume, simple to implement, and meet the insulation requirements.

3. Proposed design for multioutput isolated power supply

The isolated power supply includes the following three main sections (as shown in Figure 1).

3.1. DC-to-AC resonant inverter

The converter is a combination of a DC-to-DC buck converter and a current source resonant inverter that produces a high-frequency sinusoidal current. The power supply should generate reliable and stable output voltages in spite of the occurrence of a mains disturbance. The buck converter can select different input voltages (24, 48, or 110 DC V), which provides redundancy during the loss of one input. The power supply can

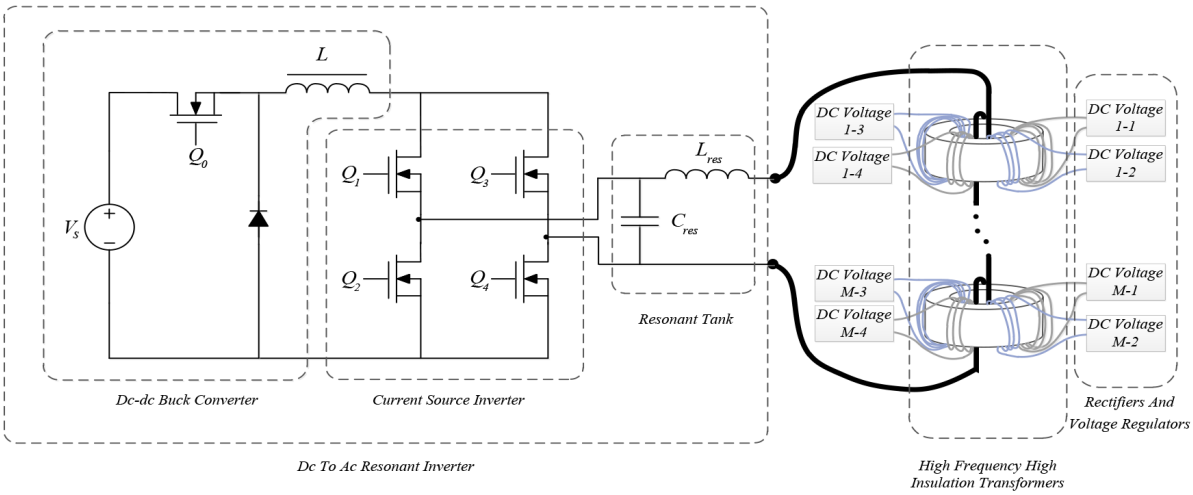

Figure 1. The entire circuit of a high-insulation scalable power supply for medium-voltage multilevel power converters.

work without any interruption in emergency situations by batteries or available DC sources. By considering these important features, this circuit is designed in two stages. The first is a buck converter acting as a current source that flows constant current into the inductor L. The second stage is an H-bridge circuit converting DC current into a high-frequency square waveform current. By using the phase shift modulation method for current source converters, which is explained and illustrated in Section 4, and assuming adequate inductance L, the H-bridge is capable of boosting the current. Therefore, by combining the buck converter and the H-bridge, a buck-boost converter with the ability to provide sinusoidal waveform current from a DC voltage source can be achieved. Moreover, embedding an adequate inductor in the first stage of the converter increases the hold-up time and is a high-reliability solution to provide sustainable power in the next stage. The resonant circuit is used to transform the square waveform current into a sinusoidal one. Resonant tank configuration is selected based on the nature of the current source H-bridge and the output rectifier capacitor filters.

3.2. High-frequency high-insulation transformers (HFHITs)

Satisfying insulation requirements at low volume with a simple structure is one of the main objectives of this article, and this can be attained using specific high-frequency transformers. A unified structure, very low mechanical hum, easy mounting, and a very low stray field make the toroid cores the desirable choice for realizing these transformers, and a single-turn high-voltage insulated cable carrying high-frequency sinusoidal current as the primary winding of the HFHITs ensures the required galvanic isolation. The secondary side of the transformers is composed of similar windings on each magnetic core, each for producing one DC supply. Since a voltage source inverter cannot balance the voltages in the HFHIT series, a current source inverter topology should be chosen.

3.3. Diode rectifier bridges and output voltage regulators

On the secondary side of each HFHIT, in order to rectify and filter the AC current to output DC voltages, a diode bridge and a capacitor are used, respectively. Due to the high frequency of the AC current, small capacitance filters are satisfactory. Regulation and overvoltage protection of the output voltages can be executed by proper utilization of Zener diodes.

4. Circuit design principles

The converter circuit components are shown in Figure 2. R_d is the equivalent resistor representing the power consumption of an IGBT gate driver circuit. V_s and I_s are the voltage and current of the secondary winding for one HFHIT, respectively. The output voltage must be constant to guarantee the correct operation of the gate driver circuits. Exact analysis of the CLL resonant converter ensures accuracy but cannot be easily used to get a handy design procedure due to the complexity of the model. Fundamental mode approximation (FMA) is a widely used method in resonant converter analysis that treats the current and voltage waveforms as pure sinusoids at a fundamental frequency and neglects other high-order harmonics [6,18]. The FMA approach gives acceptable and accurate results for operating points at and above the resonance frequency of the resonant tank. Therefore, it has been widely used when the converter works at nominal condition and frequency. FMA is valid but less accurate in the below-resonance region, and it is useful for qualitative analysis but not for an optimal design procedure [19–21].

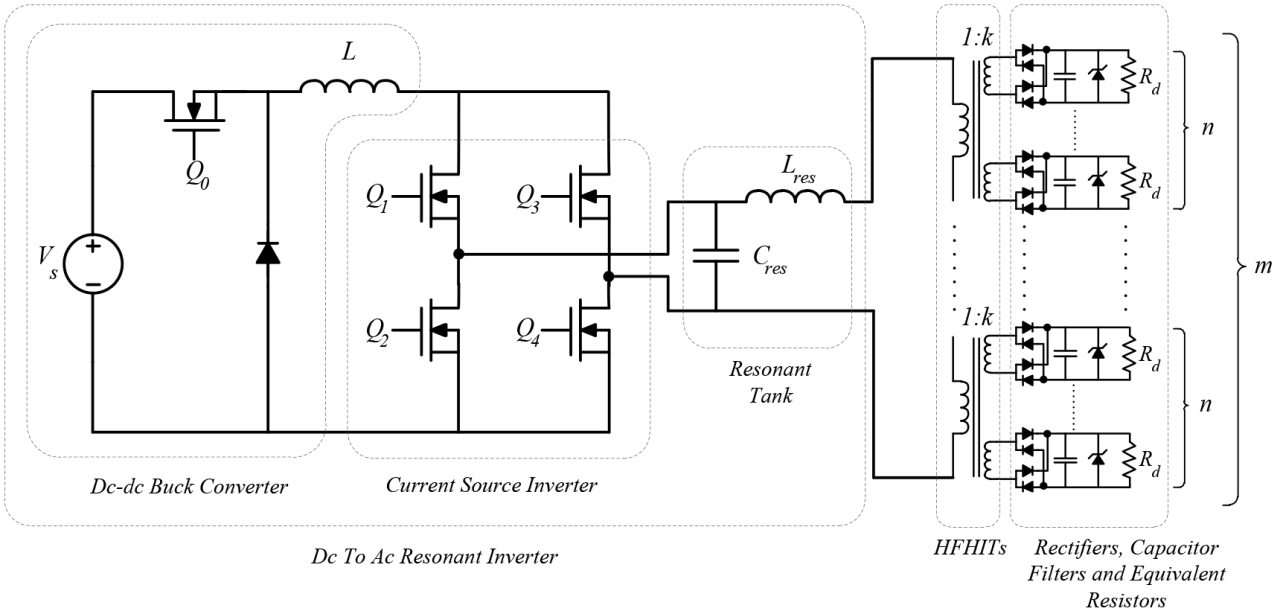

Figure 2. Equivalent circuit of the proposed high-insulation scalable power supply for medium-voltage multilevel power converters.

The AC equivalent circuit of a CLL resonant converter based on FMA analysis is shown in Figure 3. In this circuit, as most of the transferred power is subjected to the fundamental component of voltage and current, the resistance equivalent to the load and the rectifier stage are defined as follows:

$$i_{S(t)} \approx i_{S_1(t)} = I_{S_1} \sin(\omega_s t + \varphi_S); \quad v_{S_1(t)} = \frac{4}{\pi} V \sin(\omega_s t + \varphi_S); \quad R_e = \frac{V_{S_1}}{I_{S_1}} = \frac{8}{\pi^2} R_d, \tag{1}$$

where $i_{S(t)}$ is the sinusoidal current injected to the rectifier and the filter capacitor, and $v_{S1(t)}$ is the fundamental component of the secondary winding voltage. R_e is the effective resistance representing the behavior of the IGBT gate driver power consumption (see Figure 3). The effective R_e resistor is transformed to R_P, the

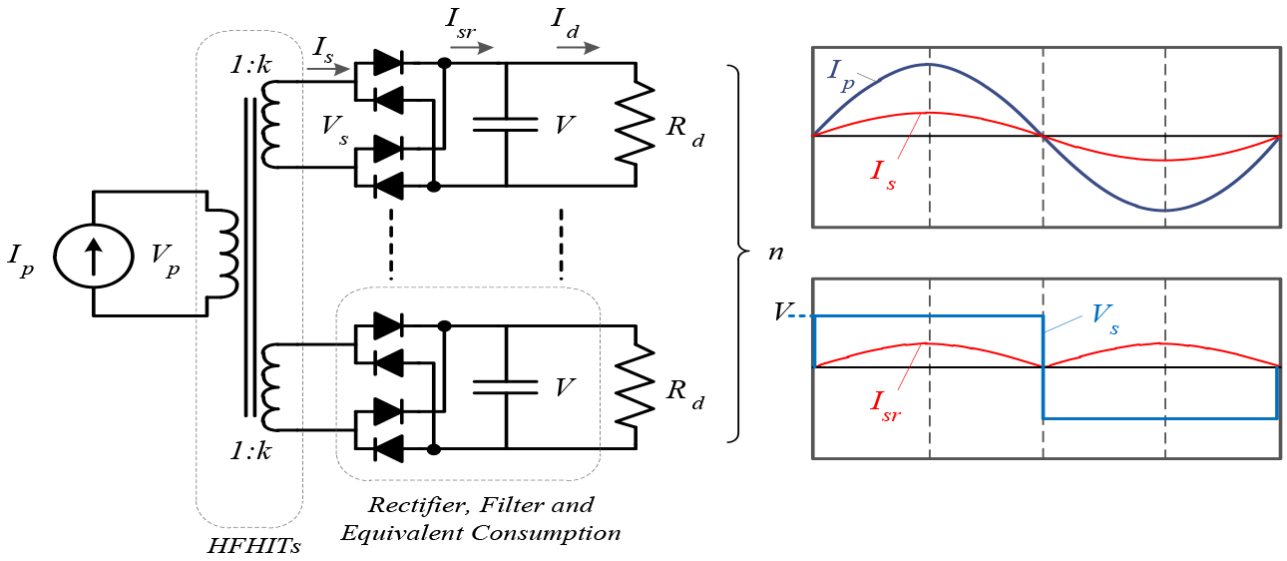

Figure 3. Equivalent circuit of the proposed high-insulation scalable power supply for medium-voltage multilevel power converters.

primary side representation resistance by the turn ratio k, and the number of secondary windings n:

$$R_P = \frac{1}{n \times k^2} R_e. \tag{2}$$

By modeling the rectifier and the power consumption, the HFHITs can be reduced to a simplified circuit composed of R_P and L_M, representing the magnetic inductance of the HFHIT. All of the HFHIT resistances and HFHIT magnetizing inductances can be respectively transferred to an equivalent resistance R_{PT} and an equivalent magnetizing inductance L_{MT} by Eq. (3):

$$R_{PT} = m \times R_P = \frac{8 \times m}{n \times k^2 \times \pi^2} R_d; \quad L_{MT} = m \times L_M; \quad L_{lT} = m \times L_l \quad . \tag{3}$$

Figure 4 shows the equivalent circuit delivered to the primary side of the HFHITs. Therefore, the resonant converter can be modeled as shown in Figure 5, where L_{SCT} is the total short-circuit inductance and L_{MT} is the total magnetizing inductance. Open-circuit and short-circuit tests should be done for the HFHITs to characterize the equivalent L_{SCT} and L_{MT} inductances. The open-circuit inductance is not dependent on the number of secondary side turns. It simply depends on the primary winding characteristics. The variation in the short-circuit inductance is very small with different secondary turns, so it is also negligible in the design. The input current $I_{CSI(t)}$ of the CL resonant tank is a square waveform current, and $I_{CSI_1(t)}$ is its fundamental component. The transfer function gain between the output equivalent voltage V and the input current $I_{CSI_1(t)}$ is defined by Eqs. (4)–(7):

$$i_{CSI_1(t)} = \frac{4}{\pi} I_{Ind.} \cos(\delta) \sin(\omega_s t), \tag{4}$$

$$\begin{aligned} G_{(\omega)} &= \left| \frac{I_{R(\omega)}}{I_{CSI_1(\omega)}} \right| \\ G_{(\omega)} &= \frac{1}{\sqrt{(1-\omega^2(L_{res}+L_{SCT})C_{res})^2 + \frac{R_{PT}^2(1-\omega^2(L_{res}+L_{SCT}+L_{MT})C_{res})^2}{(\omega L_{MT})^2}}} \end{aligned} \quad . \tag{5}$$

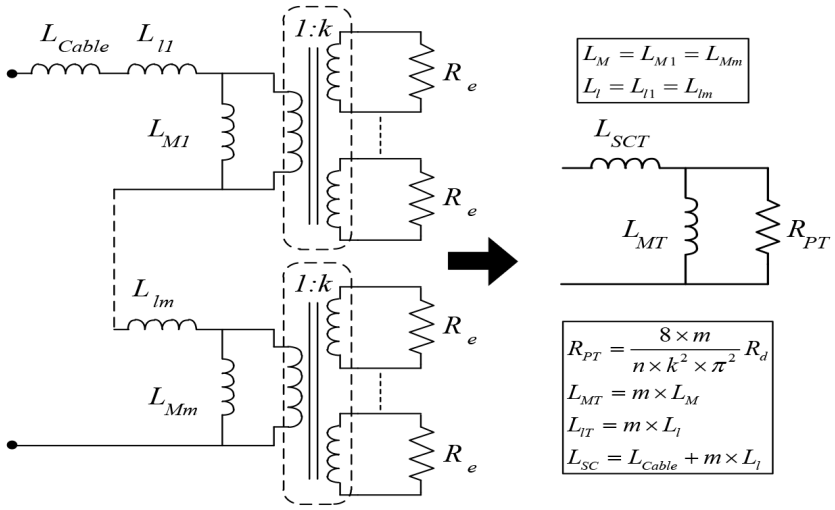

Figure 4. The equivalent circuit delivered to the primary side of the HFHITs.

In the equivalent circuit presented in Figure 5, there are two resonant frequencies due to the short-circuit inductance and the open-circuit inductance as follows:

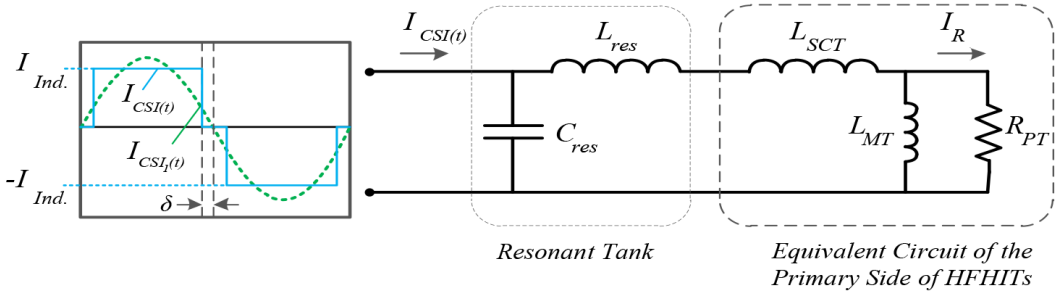

Figure 5. The equivalent circuit of the current source inverter, resonant tank, and the HFHITs.

$$\begin{matrix} \omega_{o1} = \frac{1}{\sqrt{(L_{MT}+L_{SCT}+L_{res})C_{res}}} = \frac{1}{\sqrt{(L_{OCT}+L_{res})C_{res}}} \\ \omega_{o2} = \frac{1}{\sqrt{(L_{SCT}+L_{res})C_{res}}} \end{matrix} \quad , \tag{6}$$

$$I_S = \frac{I_R}{nk}; \quad V = \frac{2}{\pi} I_S R_d = \frac{2}{\pi nk} I_R R_d; \quad G'_{(\omega)} = \left| \frac{V_{(\omega)}}{I_{CSI_1(\omega)}} \right| = \frac{2R_d}{\pi nk} G_{(\omega)} \quad . \tag{7}$$

The resonant capacitor C_r for the working frequency f_{o2} is presented in Eq. (8):

$$C_{res} = \frac{1}{(\omega_{o2})^2 (L_{SCT} + L_{res})}. \tag{8}$$

The gain bandwidth near the resonant frequency depends on the relation between $L_{SCT}+L_{res}$, L_{MT}, and the value of R_{PT}. To simplify the equation, the following assumption is made:

$$\omega_{o2} = \frac{1}{\sqrt{(L_{SCT} + L_{res})C_{res}}}; \beta = \frac{\omega}{\omega_{o2}}; Q = \frac{\omega_{o2}(L_{SCT} + L_{res})}{R_{PT}}; p = \frac{L_{MT}}{L_{SCT} + L_{res}}. \tag{9}$$

The transfer function can eventually be rewritten as:

$$|G| = \frac{1}{\sqrt{\left[\frac{1-(1+p)\beta^2}{pQ}\right]^2 + (1-\beta^2)^2}}. \tag{10}$$

Variations of p and Q change the bandwidth of the circuit. Lower p values produce higher gain and make the fixed frequency control of the CSI converter more accurate, but they reduce the bandwidth. The characteristics of the current transfer gain G versus the relevant frequency β, referring to p = 0.5, 1, and 2 for various Q values, are shown in Figure 6. For various values of β and Q, the transfer gain G has different values. For example, when $\beta = 1$ with any p, gain G would be equal to Q, and this means that the output current can be larger than the fundamental harmonic of the input current. Therefore, increasing the Q value increases the gain, and it becomes a beneficiary of a wider bandwidth.

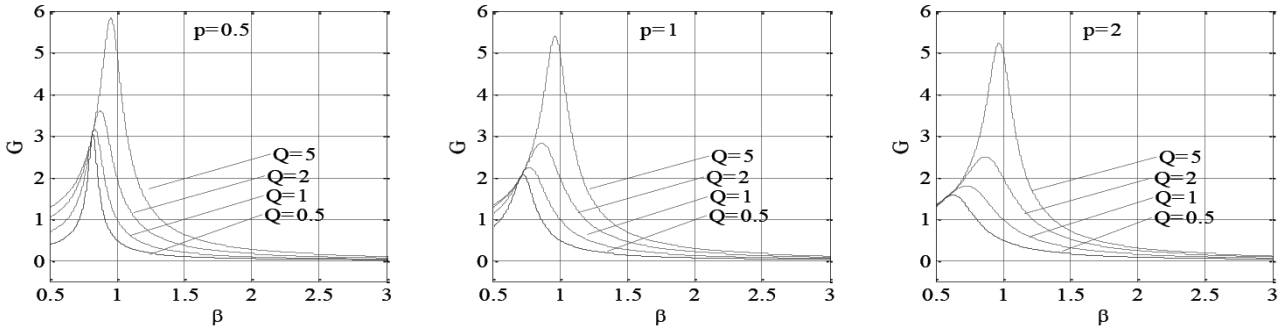

Figure 6. The curves of G vs. β referring to Q.

Furthermore, it is necessary to consider the Bode diagram for the maximum value of R_{pt} to assure that the IGBT gate drivers are correctly fed in the worst case. Due to the drift in resonant frequency because of the tolerances in passive components, a small bandwidth near ω_{o1} is not acceptable. Enough bandwidth will assure a correct circuit operation with sufficient gain, and this can be adjusted by the values of p and Q.

5. Switching strategy and control

Figure 2 shows the configuration of the converter. The duty cycle for Q_0 is D and the switches Q_1–Q_4 are complementarily switched in pairs with pulse width modulation (PWM), i.e. pairs (Q_1, Q_2) and (Q_3, Q_4). The method of phase-shifting modulation for the CSI results in different operation modes as follows:

Operation Mode I: The PWM waveform for the pair (Q_3, Q_4) lags behind that of (Q_1, Q_2) by π radians, and there is no overlap between the switches of each leg, while the duty cycle D is kept at less than 1.

Operation Mode II: The PWM waveform for the pair (Q_3, Q_4) lags behind that of (Q_1, Q_2) by less than π radians, and the overlap between the switches of each leg is 4δ in one period, while the phase shift angle θ is equal to $\pi - 2\delta$ and the duty cycle D is equal to 1, which means that the Q_0 is continually conducting.

In Operation Mode I, inductor L and switch Q_0 compose a buck converter that would produce constant current for the CSI, and the CSI provides a steady energy flow for the HFHITs. In Operation Mode II, like in Operation Mode I, inductor L works as a current source, but in this mode the converter can produce the required DC current at lower values of input voltages. In Operation Mode II, the CSI works as a boost converter from the perspective of inductor L, which is very expedient in order for the converter to keep the desired current in

the inductor when the input supply voltage drops. In fact, using these two operation modes, the isolated power supply can operate in a wide range of input voltages and output powers when facing challenging circumstances. Figure 7 shows the control system composition, where the output voltage control strategy is proposed, which can be realized by the feedback signals of the HFHIT voltages, inductor L current, and alternating Operation Modes I and II.

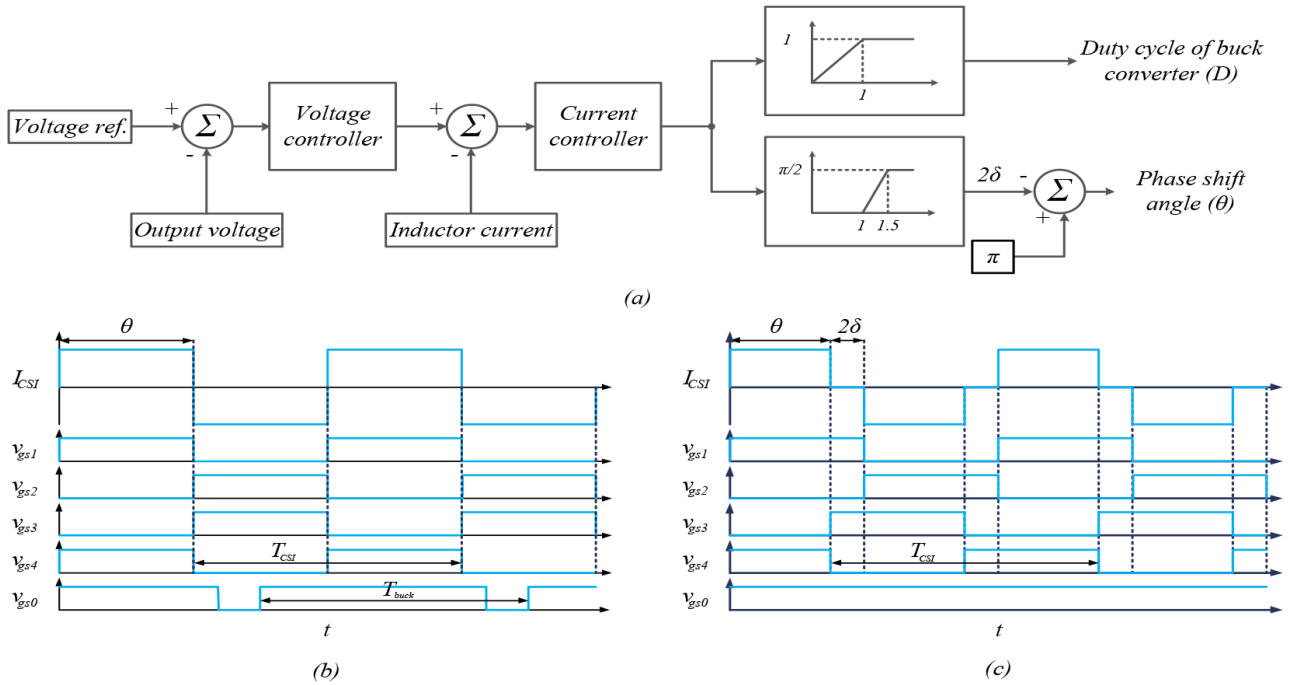

Figure 7. Block diagrams of the control system, switching commands, and operation mode of the buck converter and current source inverter: a) the overall control system, b) switching commands when the buck converter duty cycle is less than 1, c) switching commands when the buck converter duty cycle equals 1 and the current source inverter works as a boost current source inverter.

6. Simulation, experimental design, and verification

To verify the proposed power supply system, a 90-W converter was designed. The size and the weight of the converter can be reduced by increasing the switching frequency. However, it increases the loss and the temperature of the HFHIT magnetic cores, the electrical resistance of the conductors, and the switching losses. As a result, the switching and resonant frequency, with respect to the above, is selected as 31.25 kHz.

Nine HFHITs with a turn ratio of 1:11 and four similar secondary windings at each core are supposed. By considering the insulation requirements, conductor size, volume, and magnetic core weight, the HFHIT magnetic cores have been selected as pairs of TDK B64290L0048 ferrite cores. The primary winding cable insulation is XLHDPE with a 30-kV insulation level. The inductor L_{SCT}, the resonant tank elements L_{res} and C_{res}, the inductor L_{MT}, and the capacitor filter for each of the output terminals are given in the Table.

Some simulation studies are done to specify the appropriate amount of Q_e, the bandwidth, and the gain with respect to the resonant tank voltage range and the withstand voltage of the Schottky diodes. According to the L_{res}, L_{SCT}, and f_{sw} values and Eq. (8), the resonant tank capacitor calculation leads to selection of a value of 1.27 μF, but in order to establish the ZVS conditions, the capacitor should be selected to a lower value (1 μF) at a resonant frequency of 35.3 kHz. In this case, the switching frequency is less than the resonant

Table. Isolated multiple output resonant DC-to-DC converter parameters.

Parameter	Value
f_{sw}	31.25 kHz
L_{SCT}	8.3 μH
L_{res}	12 μH
C_{res}	1 μF
L_{MT}	24 μH
C_{filter}	100 μF
L	4 mH
V_S	48 V
Dead time	1 μs
Power	90 W

frequency, and the operating point is placed on the left side of the gain curve peak. According to Eq. (6), the reduction in inductance shifts the resonance frequency to a higher value than it would nominally be. By choosing the operating point to the left of the peak point in the gain curve, the possibility of creating instability in the circuit can be reduced. Simulation results at nominal conditions for the DC inductor current (i_L) and the terminal current of the H-bridge circuit are shown in Figure 8. In this case, the phase shift between the two legs of the H-bridge is π, and the buck converter controls the input current of the H-bridge and output power. The capacitor C_{res} voltage and the inductor L_{res} current are shown in Figure 9, which represents the appropriate resonant converter operation, stable resonant circuit, and sinusoidal current injection to the HFHITs. In Figure 10, the current and voltage of Q_1 of the H-bridge represent the fulfillment of the ZVS for the H-bridge switches. Figures 11 and 12 show the simulation results once the input voltage has dropped to 50% of its nominal value. In this case, the H-bridge works as a boost converter by applying phase-shift modulation (Operation Mode II), which provides the required sinusoidal current for HFHITs. Figure 13 shows that the ZVS has been established as well.

In order to verify the feasibility of the converter for providing adequate power for switching the IGBTs in a cascaded H-bridge multilevel converter, the power supply is embedded in a 250-kVA multilevel converter-based D-SSSC used for power flow control in a distribution network. Figure 14 shows the D-SSSC converter and the proposed power supplies; one of the HFHITs and the main power supply circuit are also provided in the figure. The D-SSSC converter consists of nine H-bridge cells (three cells in each phase), which provides seven-level output voltage. The high-frequency AC output current of the resonant tank flows into the nine HFHITs, whose turn ratios are 1:11. One current sensor, for DC inductor L, and a voltage sensor, in one of the output terminals, are embedded to provide feedback signals in order to control the input current of the H-bridge and output voltages. Figure 15 shows the experimental waveforms of the DC input current of the H-bridge and the terminal current of the H-bridge (similar to Figure 8 in the simulation results). Figure 16 shows the experimental waveforms of the DC input current of the H-bridge, the resonant capacitor voltage, and the resonant inductor current (the input current of the HFHITs), which are clearly sinusoidal. Moreover, the current of the resonant tank is highly sinusoid without any significant distortion or overshoot at switching instants. Figure 17 shows experimental waveforms of the output current of two secondary windings on a HFHIT and the output terminal voltages. These voltages are obviously very stable and constant during the power supply operation, and the switching of the IGBTs has no effect on the output voltages. The voltage and current of one MOSFET in the isolated power supply H-bridge are depicted in Figure 18, where the ZVS condition for the MOSFET as well as the simulations is fulfilled.

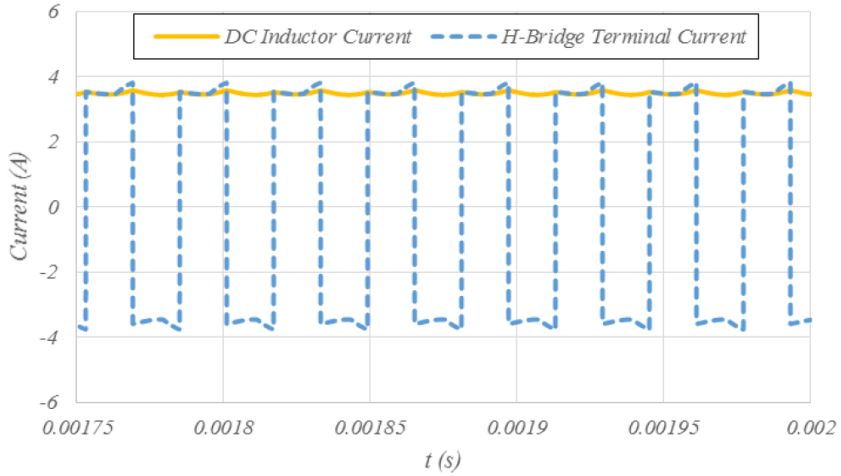

Figure 8. The inductance L current and the terminal current of the H-bridge circuit at nominal conditions.

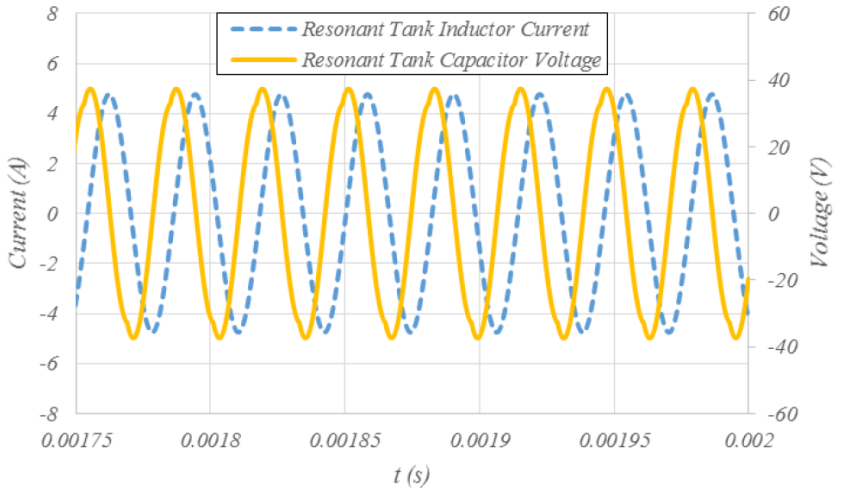

Figure 9. The capacitor C_{res} voltage and the inductor L_{res} current at nominal conditions.

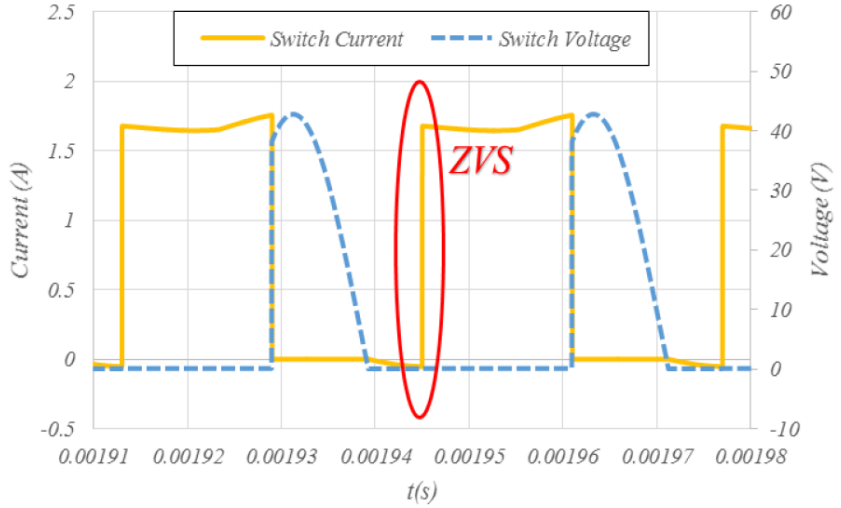

Figure 10. The current and the voltage of Q_1 at nominal conditions.

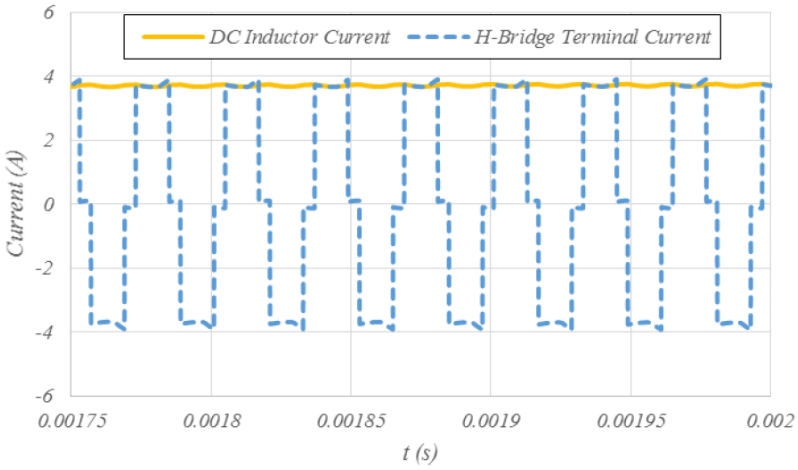

Figure 11. The inductance L current and the terminal current of the H-bridge circuit at the condition of 50% drop in the input voltage.

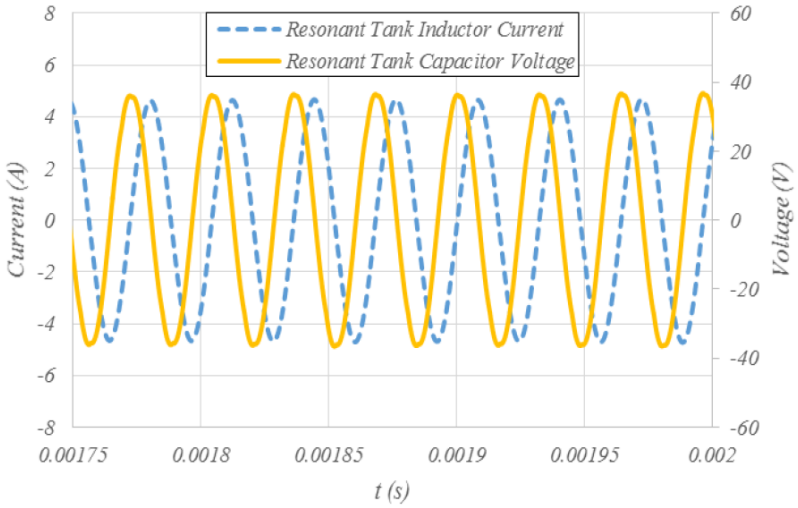

Figure 12. The capacitor Cres voltage and the inductor Lres current at a 50% drop in the input voltage.

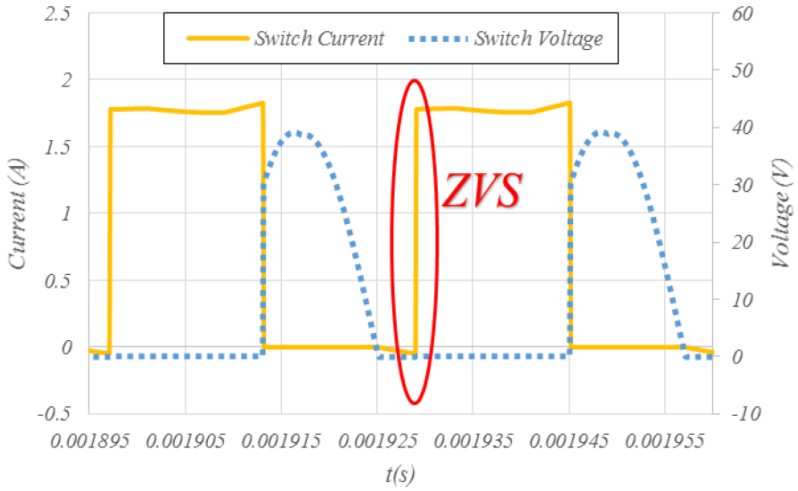

Figure 13. The current and the voltage of Q1 of the H-bridge when the input voltage is at 50% of its nominal value.

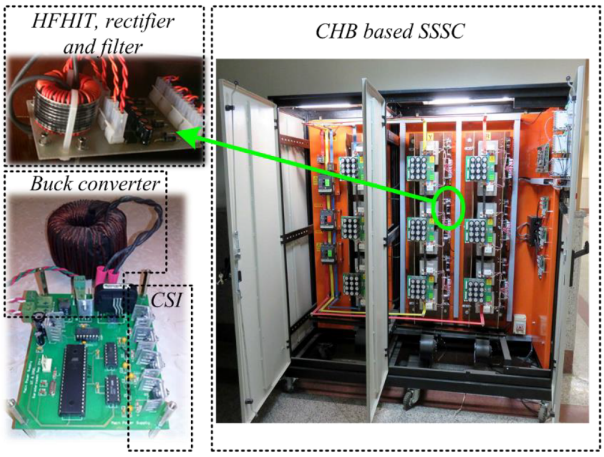

Figure 14. Constructed SSSC converter and implemented isolated multiple output resonant power supply.

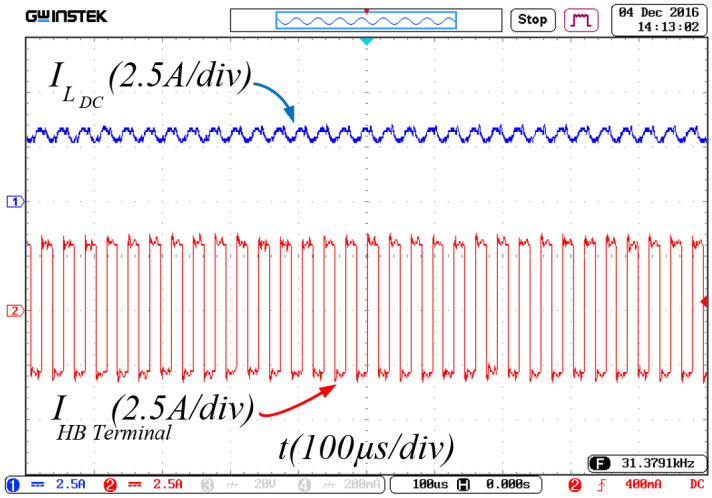

Figure 15. Experimental waveforms of the inductance L current and the terminal current of the H-bridge circuit under nominal conditions.

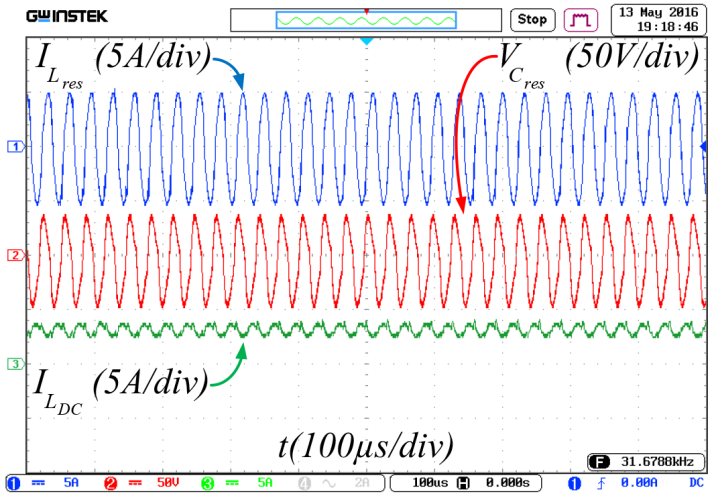

Figure 16. Experimental waveforms of the DC input current of the H-bridge, the resonant capacitor voltage, and the resonant inductor current.

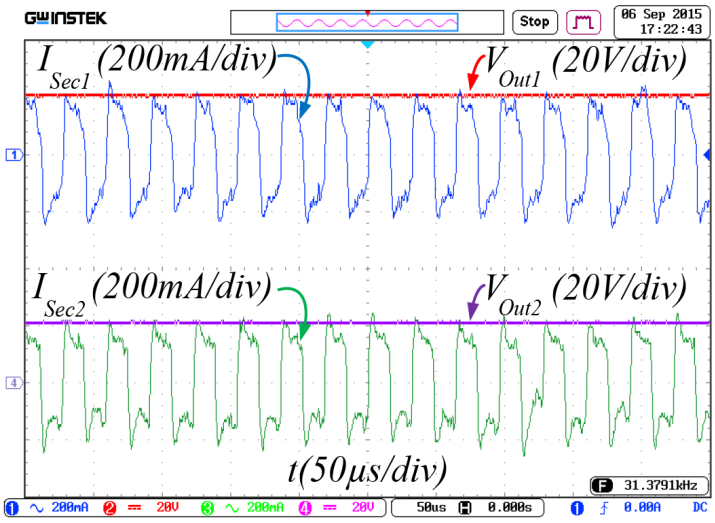

Figure 17. Experimental waveforms of the output current of two secondary windings on the HFHIT and output terminal voltages after the diode bridges and capacitive filters.

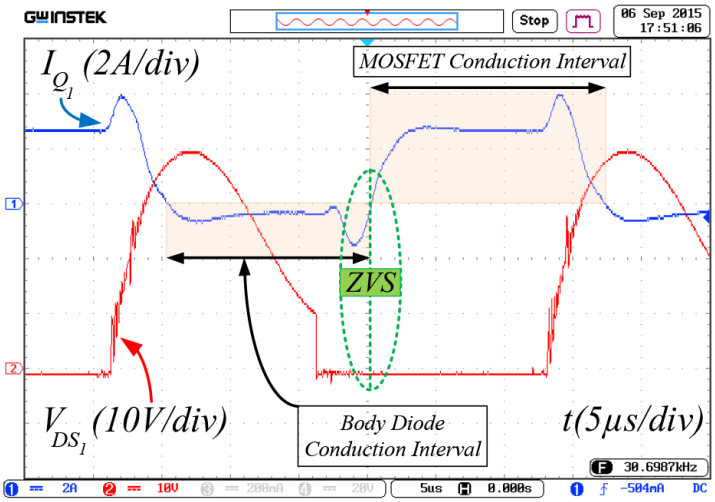

Figure 18. Voltage and current of a MOSFET in the H-bridge, and ZVS condition realization.

7. Conclusion

This paper presents a pragmatic type of isolated power supplies to provide the required power for a large number of IGBTs in a high-power multilevel converter. Two operation modes are presented for the power supply, which can guarantee constant output voltages during primary voltage supply and load variations. The proposed converter design is discussed in detail. Besides the simulation results, an experimental converter has been designed and tested on a 250-kVA D-SSSC converter. The results show remarkable agreement with the theoretical analysis in this paper and the stable operation of the power supply. In addition, due to the passive resonant tank and the proper selection of its components, the voltage stress of the resonant capacitor and loss of the HFHITs have been greatly reduced, which helps to conserve capacitor lifetime and prevent insulation aging.

Acknowledgment

This work was supported by the Iranian Power Development Company as a part of a research project called "Implementation of Scaled Static Synchronous Series Compensators Based on Multilevel Converter for Power Flow Control and Improving the Short Circuit Level Simultaneously".

References

[1] Aizpuru I, Canales JM, Fernández J. Scalable high insulation power supply for medium voltage power converters. In: 2012 International Conference on Integrated Power Electronics Systems; 6 March 2012; Nuremberg, Germany. New York, NY, USA: IEEE. pp. 1-6.

[2] Raonic DM. SCR self-supplied gate driver for medium-voltage application with capacitor as storage element. IEEE T Ind Appl 2000; 36: 212-216.

[3] Afsharian J, Wu B, Zargari N. High-voltage isolated multiple outputs DC/DC power supply for GCT gate drivers in medium voltage (MV) applications. In: 2013 Applied Power Electronics Conference and Exposition; 17 March 2013; Long Beach, CA, USA. New York, NY, USA: IEEE. pp. 1480-1484.

[4] Przybilla J, Keller R, Kellner U, Schulze HJ, Niedernostheide FJ, Peppel T. Direct light-triggered solid-state switches for pulsed power applications. In: International Pulsed Power Conference; 15–18 June 2003; Dallas, TX, USA. New York, NY, USA: IEEE. pp. 150-154.

[5] Borage M, Tiwari S, Kotaiah S. LCL-T resonant converter with clamp diodes: A novel constant-current power supply with inherent constant-voltage limit. IEEE T Ind Electron 2007; 54: 741-746.

[6] Bhat AK. Analysis and design of LCL-type series resonant converter. IEEE T Ind Electron 1994; 41: 118-124.

[7] Chuang YC, Ke YL, Chuang HS, Chen JT. A novel loaded-resonant converter for the application of DC-to-DC energy conversions. IEEE T Ind Appl 2012; 48: 742-749.

[8] Açık A, Çadırcı I. Active clamped ZVS forward converter with soft-switched synchronous rectifier. Turk J Electr Eng Co 2002; 10: 473-491.

[9] Gautam D, Bhat AK. Two-stage soft-switched converter for the electrolyser application. IET Power Electron 2012; 5: 1976-1986.

[10] Hu S, Deng J, Mi C, Zhang M. Optimal design of line level control resonant converters in plug-in hybrid electric vehicle battery chargers. IET Electrical Systems in Transportation 2014; 4: 21-28.

[11] Wu H, Mu T, Gao X, Xing Y. A secondary-side phase-shift-controlled LLC resonant converter with reduced conduction loss at normal operation for hold-up time compensation application. IEEE T Power Electr 2015; 30: 5352-5357.

[12] Shafiei N, Pahlevaninezhad M, Farzanehfard H, Motahari SR. Analysis and implementation of a fixed-frequency resonant converter with capacitive output filter. IEEE T Ind Electron 2011; 58: 4773-4782.

[13] Saradarzadeh M, Farhangi S, Schanen JL, Jeannin PO, Frey D. Application of cascaded H-bridge distribution-static synchronous series compensator in electrical distribution system power flow control. IET Power Electron 2012; 5: 1660-1675.

[14] Saradarzadeh M, Farhangi S, Schanen JL, Jeannin PO, Frey D. Combination of power flow controller and short-circuit limiter in distribution electrical network using a cascaded H-bridge distribution-static synchronous series compensator. IET Gener Transm Dis 2012; 6: 1121-1131.

[15] Malinowski M, Gopakumar K, Rodriguez J, Perez MA. A survey on cascaded multilevel inverters. IEEE T Ind Electron 2010; 57: 2197-2206.

[16] Kouro S, Malinowski M, Gopakumar K, Pou J, Franquelo LG, Wu B, Rodriguez J, Pérez MA, Leon JI. Recent advances and industrial applications of multilevel converters. IEEE T Ind Electron 2010; 57: 2553-2580.

[17] Rohner S, Bernet S, Hiller M, Sommer R. Modulation, losses, and semiconductor requirements of modular multilevel converters. IEEE T Ind Electron 2010; 8: 2633-2642.

[18] Steigerwald RL. A comparison of half-bridge resonant converter topologies. IEEE T Power Electr 1988; 3: 174-182.

[19] Beiranvand R, Rashidian B, Zolghadri MR, Alavi SM. A design procedure for optimizing the LLC resonant converter as a wide output range voltage source. IEEE T Power Electr 2012; 27: 3749-3763.

[20] Yu R, Ho GK, Pong BM, Ling BW, Lam J. Computer-aided design and optimization of high-efficiency LLC series resonant converter. IEEE T Power Electr 2012; 27: 3243-3256.

[21] Saledi S, Vahidi B, Milimonfared J, Taheri M, Moradi H. Analysis and design of an interleaved current-fed high step-up quasi-resonant DC-DC converter for fuel cell applications. Turk J Electr Eng Co 2015; 23: 2182-2196.